

1-1-1992

# Experimental implementation of MRAC for a Dc Servo Motor

Chaouki T. Abdallah

A. Cerda

R. Jordan

Follow this and additional works at: [https://digitalrepository.unm.edu/ece\\_fsp](https://digitalrepository.unm.edu/ece_fsp)

---

## Recommended Citation

Abdallah, Chaouki T.; A. Cerda; and R. Jordan. "Experimental implementation of MRAC for a Dc Servo Motor." *Proceedings of the 31st IEEE Conference on Decision and Control* (1992): 3542-3543. doi:10.1109/CDC.1992.370995.

This Article is brought to you for free and open access by the Engineering Publications at UNM Digital Repository. It has been accepted for inclusion in Electrical & Computer Engineering Faculty Publications by an authorized administrator of UNM Digital Repository. For more information, please contact [disc@unm.edu](mailto:disc@unm.edu).

## EXPERIMENTAL IMPLEMENTATION OF MRAC FOR A DC SERVO MOTOR

A. Cerda, C. Abdallah, and R. Jordan  
EECE Department, University of New Mexico  
Albuquerque, NM 87131, USA

### ABSTRACT

This paper describes a hardware implementation of adaptive controllers using a Digital Signal Processor (TMS320C25). The research explores two model reference adaptive control schemes and some of the practical problems associated with their implementation.

### 1 Introduction

Our research explores model reference adaptive control (MRAC) schemes in a real system. The motivation being that although the theory of adaptive control is highly developed, its practice has been limited [3]. We successfully implemented two MRAC schemes to control a DC servo motor using a digital signal processor. In addition, we studied the following practical aspects of adaptive control:

1. The existence of "Limit Cycles" in the adaptive gains.
2. The influence of the  $\gamma$  modification.
3. The influence of the external input.

Other effects were also studied as described in [1] but are not included in this short paper. Additionally, we derived and implemented a new controller that adjusts the  $\gamma$  in the application of the  $\gamma$  modification [3].

### 2 Hardware Implementation

The overall system - plant, controller, and display block - is shown in Figure 1. The plant is a DC servo motor. The controller includes

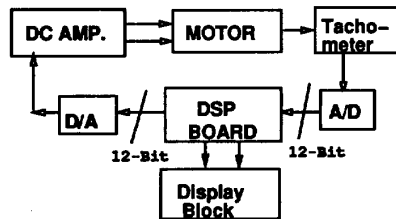


Figure 1: Block Diagram of the Physical System

the hardware (A/D, DSP board D/A, DC power amplifier, etc.) and the software that implements the adaptive controllers. The display block contains the parallel port, D/As, oscilloscopes, etc. and the software necessary to display some signals in real time [1].

### 3 Software Implementation of the controllers

The TMS320C25 is a fixed-point microprocessor so that in our experiments filters, difference equations, sine wave generations and random sequences are implemented using  $Q$  formats [2].

In our experiments, the plant is given by  $K_p/(s+P_p)$ , the desired model is  $K_m/(s+P_m)$ , the output of the plant is  $y_p$ , that of the model is  $y_m$ , the input to the plant is  $x_p$  and that of the model is  $x_m$ . The error is defined as  $e_1 = y_p - y_m$ . All assumptions for the existence of a stable adaptive controller as described in [3] are satisfied. Equation (1) constitute the adaptive law to adjust the proportional gain [3] for case 1, where only the high frequency gain is unknown: Equation (2) is the discrete version of this law, obtained

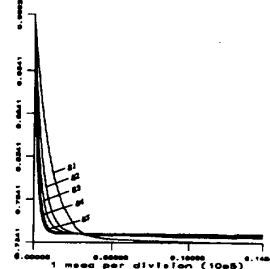


Figure 2:  $kt$  vs time when  $\gamma = 10, 20, 30, 40$ , using the backward approximation [4], where  $h$  is the sampling time,

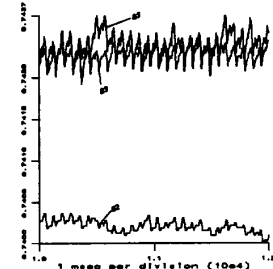


Figure 3:  $kt$  vs time when  $\gamma = 20, 30, 50$

$$\dot{kt}(t) = -\gamma \cdot \text{sgn}(K_p) \cdot e_1(t) \cdot x_m(t) \quad (1)$$

$$kt(i) = -\gamma \cdot \text{sgn}(K_p) \cdot h \cdot e_1(i) \cdot x_m(i) + kt(i-1) \quad (2)$$

Equations (3) and (4) represent the adaptive laws of case 2 where both the high frequency gain and the pole are unknown [3]. Equations (5), and (6) are the discrete time implementations.

$$\dot{kt}(t) = -\gamma \text{sgn}(K_p) \cdot e_1(t) \cdot x_m(t) \quad (3)$$

$$\dot{th}(t) = -\gamma \text{sgn}(K_p) \cdot e_1(t) \cdot y_m(t) \quad (4)$$

$$kt(i) = -\gamma \text{sgn}(K_p) h e_1(i) x_m(i) + kt(i-1) \quad (5)$$

$$th(i) = -\gamma \text{sgn}(K_p) h e_1(i) y_p(i) + th(i-1) \quad (6)$$

### 4 Experimental Results

#### 4.1 $K_p$ Unknown case

The first set of experiments were designed using equation (2) to study the effect of  $\gamma$ . We found that  $\gamma$  has a dual function in our experiments; it makes the convergence possible by eliminating the limit-cycle effect due to truncation, and it increases the convergence speed of the gains. Figure 2 shows the convergence of the gain  $K_p$  for different  $\gamma$ 's. There is an important trade-off in the use of  $\gamma$ ; A large  $\gamma$  produces large oscillations of the adaptive parameter(s). Figure 3 shows the oscillations around the final values for 3 different  $\gamma$ 's.

The other important study performed using the  $K_p$  unknown case examined the influence of the input on the convergence of  $kt$ . Figure 4 shows the convergence of  $kt$  for 6 different step inputs. A

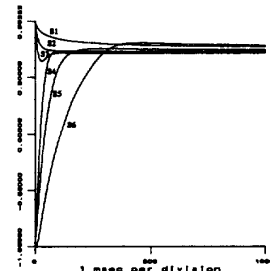


Figure 4:  $kt$  vs time [S1 :  $kt = 1, x_m = -2.5$  S2 :  $kt = 1, x_m = -5$  S3 :  $kt = 1, x_m = -7.5$  S4 :  $kt = -1, x_m = -2.5$  S5 :  $kt = -1, x_m = -5$  S6 :  $kt = -1, x_m = -7.5$ ]

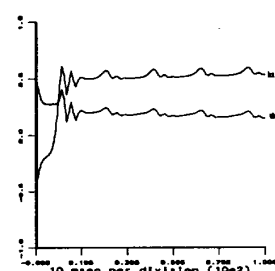


Figure 5: A Close Look at  $kt$  and  $th$

larger magnitude step is shown to produce a faster convergence of the adaptive parameter.

#### 4.2 $K_p$ and $P_p$ Unknowns Case

In the second case, two adaptive gains were adjusted using equations (5) and (6). The input to the model used in this study is a sinusoidal wave form. The amplitude of this sinusoid was adjusted experimentally to make the convergence of  $kt$  and  $th$  possible. The DC value of the sinusoid was set to avoid an input which crossed the level of 0 Volts in order to avoid the nonlinear region of the motor [1]. One of the models used to test the controller (*model1*) was :

$$G_m(s) = \frac{100}{s + 100}, \quad (7)$$

During the first second of operation, the controller adjusted a large portion of the parameters ( $kt$ , and  $th$ ). Figure 5 shows 1 second of the trajectory of  $kt$  and  $th$ , and Figure 6 shows the first 600 msecs of the trajectories of  $y_m$ ,  $y_p$ , and  $e_1$ .

An effect similar to the one obtained by updating only  $K_p$  was observed in this case. The speed of convergence is related to the magnitude of  $\gamma$ , as is the oscillatory behavior of the parameters. Figure 7 provides a close look at the oscillations in one of the parameters after 20 secs of operation of the controller. The curve C2k1 corresponds to a  $\gamma$  of 50, C2k2 corresponds to a  $\gamma$  of 100, and C2k3 corresponds to a  $\gamma$  of 200. Increasing the convergence speed has one drawback; it creates more oscillations in the gains.

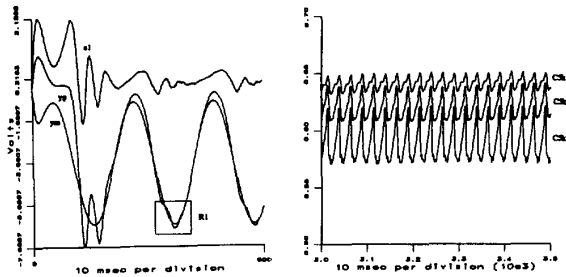


Figure 6: A Close Look at  $y_m$ ,  $y_p$ , and  $e_1$  Figure 7: Close Look of  $kt$  oscillations for  $\gamma = 50, 100, 200$

#### 4.3 Adjusting $\gamma$

The ( $\gamma$ ) modification increases the speed of convergence significantly, but it produces an oscillatory behavior around the final value of the adaptive gains. A filter was designed to adjust  $\gamma$  as a function of the output error  $e_1$ . Figure 8 shows a block diagram of this filter. The first block represents a low-pass filter followed by a rectifier that finds the absolute value of the filter output. This value is multiplied by a constant term

The new controller runs for 18 secs using a fixed  $\gamma$  as the previous controller did. Then the subroutine that implements the  $\gamma$  filter is called every 500  $\mu$ secs and the process of adjusting the factor  $\gamma$  begins. The results obtained by using this controller can be observed

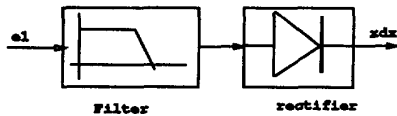


Figure 8: Adjustment of  $\gamma$  esquematic block

in Figure 9 ( $kt[0] = -0.5$ ,  $th[0] = 0.5$  and initial  $\gamma = 200$ ). The trajectories that the parameters follow in both plots is similar. The gains  $kt$  and  $th$  converge to constant values, and the oscillation in the gains disappear.

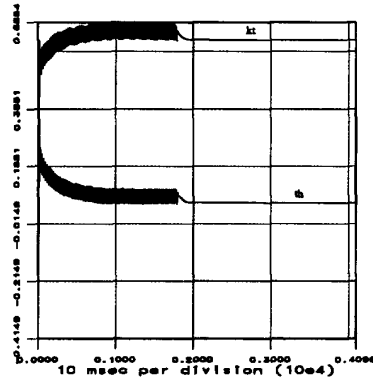


Figure 9: Parameter Trajectories for  $kt[0] = -0.5$  and  $th[0] = 0.5$

## 5 Conclusions

The effect of finite register length in digital signal processing is an important factor to consider when a controller is implemented using

a fixed-point microprocessor. In our case, the truncation that occurs when a 32-bit hardware register is stored in a 16-bit memory location, is one of the main factors of the *limit cycle* present in the convergence of the adaptive gains. The solution to this problem was to use the  $\gamma$ -modification. The  $\gamma$  modification which has commonly been used to increase the speed of convergence in computer simulation, actually has a dual function in our experiments; it makes the convergence possible, and it can be used to increase the convergence speed of the gains. A larger  $\gamma$  produces a faster convergence of the parameters, but unfortunately, the adaptive gains oscillate around the expected final value.

A special controller was designed and implemented to adjust  $\gamma$  as a function of the output error  $e_1$ . This controller reduces the oscillations of the adaptive gains around the final value.

Finally, the magnitude of a step input was shown to have an important influence on the time of convergence of the adaptive gain.

## References

- [1] A. Cerda. *A Digital Signal Processor Implementation of a Model Following Adaptive Controller for a DC Servo Motor*. MS Thesis, EECE Department, University of New Mexico, Albuquerque, NM, 1992.
- [2] Texas Instruments. *Digital Control Applications with the TMS320 Family*. Digital Signal Processing Products, TI, Houston, Texas, 1st edition, 1991.
- [3] K. Narendra and A. Annaswamy. *Stable Adaptive Systems*. Prentice-Hall, Inc., Englewood Cliffs, N.J., 1st edition, 1989.
- [4] C. Phillips and H. Nagle. *Digital Control Systems*. Prentice Hall, Englewood Cliffs, New Jersey, 2nd edition, 1990.